Bulletin of the Seismological Society of America, Vol. 81, No. 6, pp. 2441–2457, December 1991

LATERAL VELOCITY VARIATIONS IN THE ANDEAN FORELAND IN ARGENTINA DETERMINED WITH THE JHD METHOD

By J. Pujol, J. M. Chiu, R. Smalley, Jr., M. Regnier, B. Isacks, J. L. Chatelain, J. Vlasity, D. Vlasity, J. Castano, and N. Puebla

Abstract

Lateral velocity variations in the Andean foreland near San Juan Province, Argentina, were detected by analyzing the station corrections computed as part of the joint location of local earthquake data. The events, recorded by a portable network (PANDA), have intermediate and shallow depths (about 100 km and less than 40 km, respectively). The JHD technique was applied to intermediate-depth events and to two subsets of shallow events that concentrate on two distinct geologic units (Precordillera and Pampean Ranges). The computed station corrections have a strong dependence on the data processed. Analysis of the different patterns of corrections shows that the corrections are consistent with the presence of large-scale lateral velocity variations bounded by major fault systems. Based on these corrections, a qualitative velocity model is proposed that has relatively high velocities between the eastern Precordillera and a westerly dipping plane on the eastern edge of Pie de Palo (one of the mountain blocks of the Pampean Ranges). Velocities are lower immediately east of this plane and between the central and eastern Precordillera. This model has important tectonic implications, because it suggests that there is a major boundary between the central and eastern Precordillera and that the Pampean basement, whose extent is unknown, underlies the eastern Precordillera. The existence of large velocity variations across the Precordillera is consistent with a westward shift of almost 10 km of the relocated intermediate-depth events and with the removal of an apparent westward dip (opposite to the direction of subduction) observed in the Wadati–Benioff zone as determined from single-event location. The analysis of the intermediate-depth events also exemplifies the deleterious effect on the JHD results introduced by the cancellation of small singular values in the computation of the station corrections.

Introduction

In two recent articles, the relation between JHD stations corrections and velocity anomalies was discussed. Pujol *et al.* (1989b) suggested that an unusual earthquake swarm in eastern Arkansas, in a region considered to be aseismic, could be related to the presence of a low-velocity zone in the swarm area. Although this hypothesis was consistent with other geophysical information, it could not be independently verified. Pujol and Aster (1990), however, analyzed swarm events from the Phlegraean Fields, a complex volcanic area near Naples, Italy, and found that the pattern of station corrections was consistent with the presence of the low-velocity zone determined by the 3-D velocity inversion of the same data set (Aster and Meyer, 1988).

The analysis of the Phlegraean Fields data shows beyond doubt the usefulness of the station corrections in giving qualitative information about localized velocity variations. The question is whether lateral velocity changes across a seismic network can also be detected. The answer, in principle, is yes, provided

that the seismic events are relatively clustered, so that the ray path from each of the events to any given station is approximately the same. In this way, the station corrections represent not only departures from the velocity model near the stations, but also near the source and along the ray paths. Therefore, it can be expected that in some circumstances the pattern of station corrections will reveal the gross lateral velocity variations under a network.

The JHD technique was applied to data collected by a portable network (PANDA) in the Andean foreland in San Juan Province, Argentina. The area is characterized by a rather complicated, and not fully understood, tectonic setting and by crustal (5 to 40 km) and intermediate-depth (about 100 km) seismicity. The shallow seismicity is primarily associated with two clearly distinguishable geologic units, while the deeper seismicity is related to the subduction of the Nazca plate. This variety of hypocentral locations was ideal, because the station corrections computed for various subsets of events showed patterns strongly dependent on the data analyzed, which in turn were associated with large lateral velocity variations.

The JHD method used in this article was developed by Pavlis and Booker (1983) and was later modified by Pujol (1988). This modification increased the speed of the computations substantially, and at the same time provided some insights into the method itself, which are very useful in the interpretation of the results. Of particular importance are the singular values of a square matrix $\mathbf{S}^T\mathbf{S}$, whose generalized inverse is directly related to the computation of the station corrections. One of the singular values is identically zero and, if no other singular value vanishes, then the JHD solution is unique. Nonzero but relatively small singular values indicate the possibility that this uniqueness is lost. Further details of the technique have been given elsewhere (Pujol, 1988; Pujol *et al.*, 1989b; Pujol and Aster, 1990).

Tectonic Setting and Data Acquisition

The Andean mountain system can be subdivided into large-scale segments that are strongly correlated with the angle of subduction of the Nazca plate (Stauder, 1973, 1975; Baranzangi and Isacks, 1976, 1979; Isacks and Baranzangi, 1977). Our study area (Fig. 1) is above the portion of flat subduction between 27° and 33°S, which is characterized by an almost horizontal Wadati-Benioff zone over as much as 200 km in an east-west direction (Smalley and Isacks, 1987; Vlasity, 1988). Within the segment of subhorizontal subduction, the Andean foreland consists of the Precordillera and the Pampean Ranges (Figs. 1 and 2), which correspond to thin-skinned and thick-skinned tectonic styles, respectively. Since the tectonics of the region has been well summarized by Fielding and Jordan (1988), only a brief description, based on this reference, will be given here.

The Precordillera is a Neogene to Quaternary thin-skinned thrust belt about 300 km long and subdivided into three parallel subprovinces: western, central, and eastern Precordillera. The western Precordillera is outside the network and therefore will not be considered further.

The central Precordillera is characterized by imbricate thrust faults accompanied by west-dipping folds. The decollement is estimated to vary from 3 to 4 km below the surface in the eastern part of the central Precordillera to 5 to 8 km in the western part. Crystalline basement is not exposed in the central Precordillera. The surface structures in the eastern Precordillera are imbricate

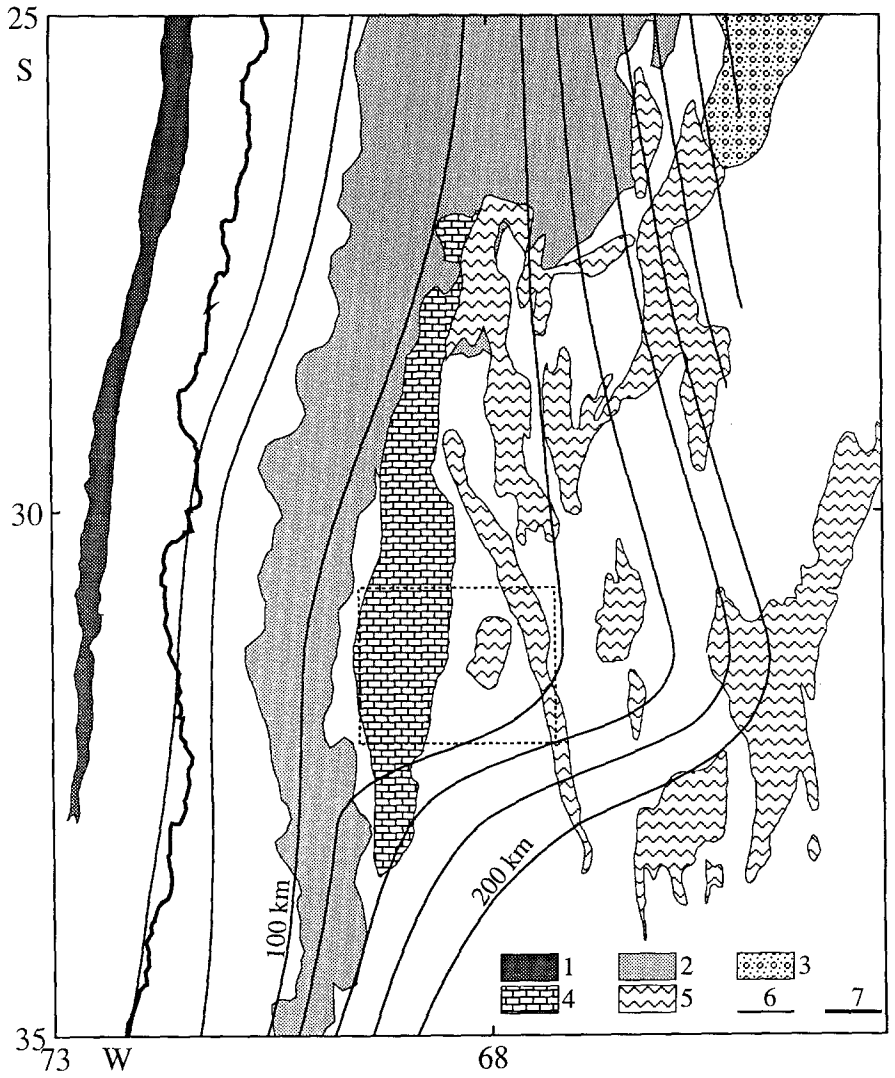

FIG. 1. Map of southwestern South America showing the major tectonic features and the study area (indicated by the dashed box). Key to symbols: (1) trench, (2) elevation higher than 3 km, (3) Santa Barbara range, (4) Precordillera, (5) Pampean ranges, (6) contours of the Wadati-Benioff zone, (7) coastline. After Isacks (1988) and Jordan *et al.* (1983).

east-dipping thrust faults to the south and large-scale folds to the north. This difference is thought to be the result of different erosional levels rather than the result of changes in tectonic style along strike. The presence of a Devonian melange on the eastern side of the eastern Precordillera has been interpreted as an indication of an accreted terrane (Ramos *et al.*, 1986).

The boundary between the central and eastern Precordillera is the Matagusanos valley. The depth to the basement under the valley is estimated to be between 8 and 10 km. This estimation is based on information obtained from a borehole (Fig. 2) drilled by the Argentine National Oil Company (YPF) to a depth of 6 km and from the downward projection of the stratigraphy. Most of the crustal seismic activity in the Precordillera takes place in the basement under the Matagusanos valley (Smalley *et al.*, 1988; Smalley and Isacks, 1990).

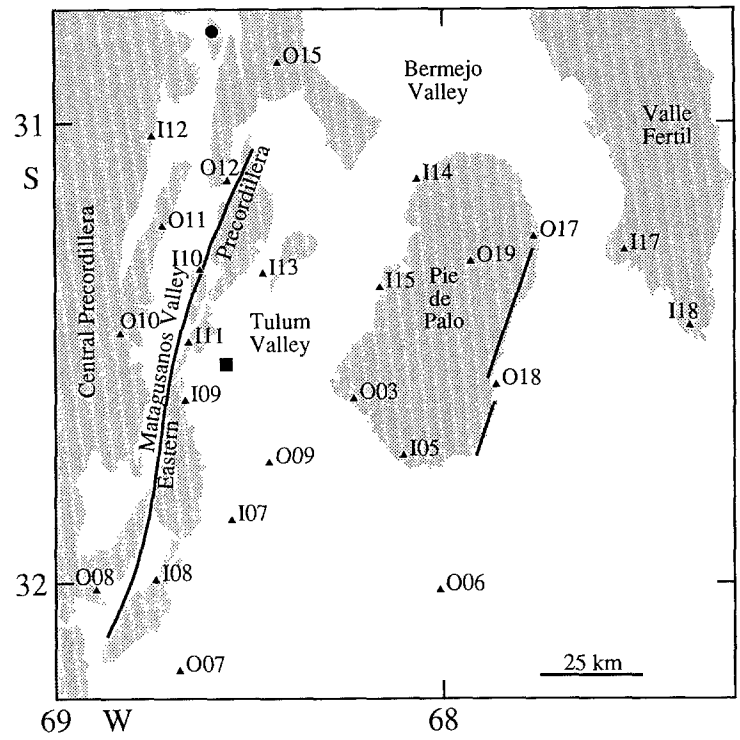

FIG. 2. Location of the PANDA stations (solid triangles) and major tectonic features in the area covered by the network. One of the stations is out of the boundaries of the map and was not used in the joint location. The central recording site was the INPRES building in San Juan city (indicated by the solid box). The heavy lines correspond to mapped reverse faults (Langer and Bollinger, 1988) relevant to this article. Shaded areas correspond to mountains, and white areas correspond to sedimentary basins. The faults on Pie de Palo dip to the west. The fault east of the Matagusanos valley dips to the east and in the text is referred to as the Matagusanos fault. The solid circle indicates the location of a 6-km-deep borehole.

To the east of the Precordillera lie the uplifted Precambrian basement blocks of the Pampean Ranges. The blocks are bounded by reverse faults trending primarily in the north–south direction and dipping to the east or the west. It should be noted that although the eastern Precordillera has traditionally been considered part of the thin-skinned tectonics, it may be more appropriate to treat it as part of the Pampean Ranges (Allmendinger *et al.*, 1990; Smalley *et al.*, 1991).

The Pie de Palo mountain block is characterized by high crustal seismic activity (Regnier *et al.*, 1988; Smalley and Isacks, 1990), which includes the M_S = 7.3 Caucete event of 1977 (Volponi, 1979; Kadinsky-Cade *et al.*, 1985; Langer and Bollinger, 1988). To the northeast of Pie de Palo is the Valle Fertil range, bounded to the west by a reverse fault dipping about 30° to the east. The Bermejo valley separates Valle Fertil from Pie de Palo and the eastern Precordillera. North of Pie de Palo, this valley is filled with 6 km of Cenozoic strata on the western side and probably more on the eastern side (Fielding and Jordan, 1988).

The Tulum valley, which separates Pie de Palo from the Precordillera, is relatively shallow (1 to 2 km) and covers the contact between the basement of

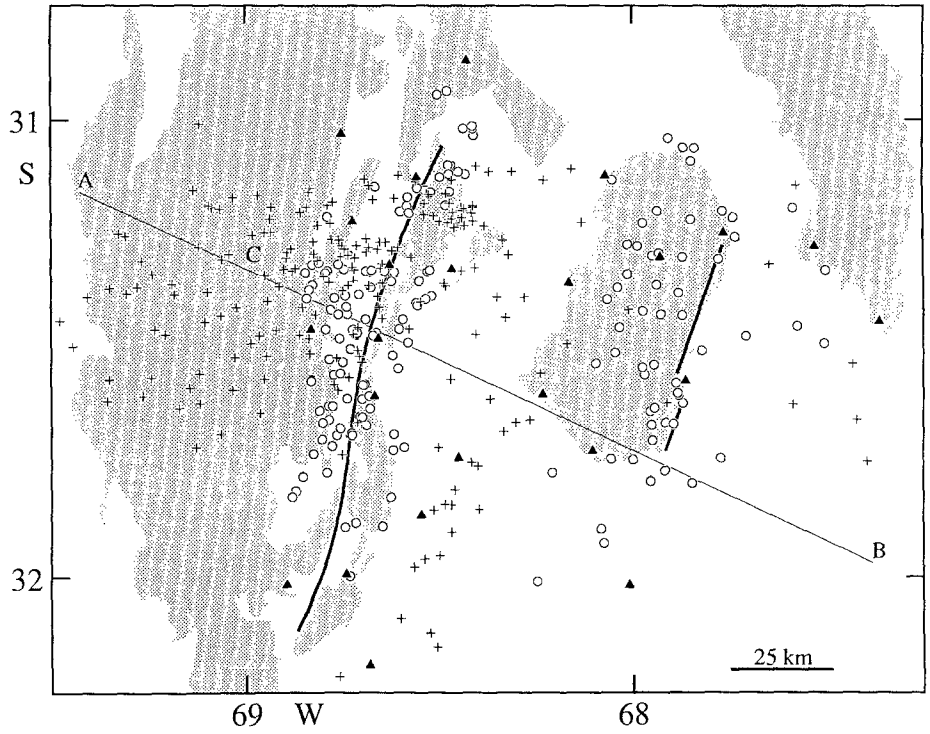

FIG. 3. Shallow (open circles) and intermediate-depth (crosses) events analyzed in this study (JHD locations). These events do not reflect the actual seismicity, which covers a wider area, but for reasons discussed in the text they were considered best suited for JHD studies. There are 200 intermediate-depth events, 116 shallow events under the Matagusanos Valley, and 59 events under and near Pie de Palo. Lines AB and CB indicate cross sections shown in Figures 4, 7, and 9.

the Pampean Ranges and that beneath Paleozoic units of the eastern Precordillera. The westernmost exposures of basement similar to that of Pie de Palo are found in small outcrops 10 km to the east of the eastern Precordillera (stations I07, O07, and O09, (Fig. 2) are located on these outcrops).

The data used in this study (Fig. 3) are a subset of the data collected from September 1987 to May 1988 by the PANDA stations, which were deployed in the Andean foreland in the vicinity of the city of San Juan, Argentina (Fig. 2). PANDA consists of 40 three-component stations with overlapping high- and low-gain channels transmitted via analog FM radio to a central recording site where a multi-station triggering algorithm is used to detect and identify earthquakes for digital recording at 0.01 sec. To overcome limitations imposed by the topography, half of the stations are used as repeaters (Chiu *et al.*, 1991).

In San Juan Province, PANDA occupied 25 stations sites (Fig. 2). The remaining stations were used to form small arrays at three of the sites (O03, I05, I13). The selection of the station locations was dictated by logistics and the need for repeater sites. All stations but two (O06, O12) were on hard rock. The station site lithology and elevation are given in Table 1.

DATA ANALYSIS

As mentioned in the Introduction, we are interested in analyzing events with rather restricted spatial locations. Therefore, the events under and near Pie de

TABLE 1

Station	Elevation (m)	Lithology
O03	625	basement
I05	754	basement
O06	550	unconsolidated sediments
I07	837	basement
O07	843	basement
I08	1210	sedimentary rock
O08	1589	sedimentary rock
I09	985	sedimentary rock
O09	703	basement
I10	1311	sedimentary rock
O10	1468	dacite
I11	1020	sedimentary rock
O11	1060	sedimentary rock
I12	1490	sedimentary rock
O12	1164	alluvium
I13	712	travertine
I14	998	basement
I15	996	basement
O15	923	sedimentary rock
I17	1022	basement
O17	884	basement
I18	726	basement
O18	831	basement
O19	3165	basement

Palo, the Matagusanos valley events, and the intermediate-depth events were considered separately.

The velocity model for the area was taken from Bollinger and Langer (1988), who improved an earlier velocity model (Volponi, 1968) by incorporating refraction data supplied by YPF and data collected by a temporary network deployed to record aftershocks of the 1977 Caucete earthquake. The depth to the top of the mantle and the mantle velocity had been determined by Castano (unpublished data) from surface-wave studies. Bollinger and Langer's model has four layers, with the first one corresponding to the sedimentary cover in the Tulum and Bermejo valleys. However, since only one of the PANDA stations (O06) was located on soft sediments, this layer was ignored. The model adopted here consists of three layers with thicknesses of 10, 22, and 13 km and *P*-wave velocities of 5.88, 6.2, and 7.3 km/sec, respectively, over a half-space with a velocity of 8.1 km/sec. An average V_p / V_s ratio of 1.75 was used.

In areas with large variations in topography, like San Juan Province (Table 1), it is important to incorporate station elevation into the JHD computations. One approach is to assume that all the stations are at the same elevation and then to proceed in one of the following two ways. One way is to correct the arrival times to a reference depth by assuming vertical incidence at each station (a typical approach with most single-event location programs); but because this assumption is not always correct and can bias the computations, this method is not used here. The other way is to carry the computations using the raw arrival times, so that the station corrections account for all the contributions to the travel-time residual for a given station. This approach is reasonable when the

main purpose of the JHD is to get more reliable event locations, but it is not appropriate to interpret the station corrections. Since the latter is the most important goal of this article, we modified the location part of the JHD program to take into account the actual elevation of each station.

The comparison between the results of single-event location and joint location requires some comments. In most standard location programs, arrival times for far stations and for stations with large residuals are weighted down regardless of the quality of the arrival. On the other hand, in our JHD computations such additional weighting is not introduced. Therefore, for comparison purposes, we locate each event with a simple least-squares program that only allows for quality weighting. The program also takes into account actual station elevations, although it is possible to apply travel-time corrections. In the following sections, reference to single-event locations will imply locations obtained with this program.

Pie de Palo Events

First, only events directly under Pie de Palo (Figs. 3 and 4) were used in the joint location. In this case, the smallest nonzero and largest singular values of $\mathbf{S}^T\mathbf{S}$ were equal to 0.4 and 54, respectively, so that $\mathbf{S}^T\mathbf{S}$ was well conditioned. The *P*-wave station corrections (Fig. 5a) show a clear pattern of positive and negative values associated with Pie de Palo and the Precordillera. Except for station O19, the corrections for Pie de Palo stations located west of the eastern fault are negative and close to each other, an indication that along the different raypaths the medium is rather homogeneous. The corrections for the two eastern stations (O17, O18) are different from each other and from the other corrections.

For the Precordillera stations, those east of the Matagusanos fault (Fig. 2) have negative corrections, while stations west of the fault have relatively large positive corrections.

The average travel-time RMS residual was 0.26 sec for the single-event locations and decreased to 0.14 sec after relocation. The relocated hypocenters moved, on average, 0.7 km to the north, up to ± 1 km in an east–west direction, and became 1.3 km deeper.

When events under and in the vicinity of Pie de Palo (Figs. 3 and 4) were used in the joint location, the magnitude of the corrections for the Precordillera stations (Fig. 5b) varied little with respect to the previous values. For the Pie de Palo stations, however, the corrections for the two eastern stations (O17, O18) changed substantially, becoming even more different from the other corrections

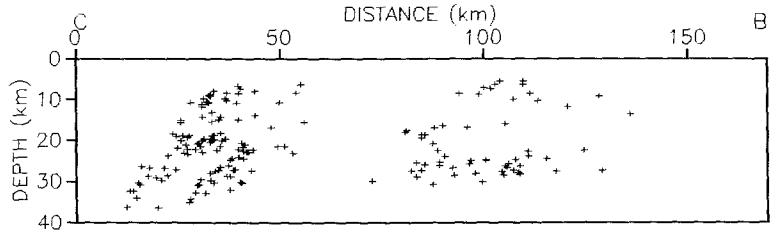

FIG. 4. Depth cross section for the shallow events (for location see Fig. 3).

than they were before. In addition, the correction for station O19 became somewhat larger. This behavior of the corrections is discussed later. The smallest nonzero and largest singular values of $\mathbf{S}^T\mathbf{S}$ were 0.8 and 67, respectively. The average RMS residual decreased from 0.27 to 0.16 sec after relocation. The changes in hypocentral location were somewhat different from those obtained for the previous data set; on average, the relocated epicenters moved 1 km to the east and 0.4 km to the north, and depths increased by 1.6 km.

Matagusanos Events

For these events (Figs. 3 and 4) the smallest nonzero and the largest singular values of $\mathbf{S}^T\mathbf{S}$ were equal to 0.7 and 71, respectively. The *P*-wave station corrections (Fig. 6) show some differences with respect to those obtained for the Pie de Palo events. For the Pie de Palo and Valle Fertil stations, all corrections are negative. For stations west of the Matagusanos fault, the corrections are consistently positive and of rather large magnitude (on the order of 0.5 sec). On the other hand, the corrections for stations east of the fault but west of Pie de Palo are negative or positive with small absolute values. On average, the RMS residual decreased from 0.30 to 0.19 sec after relocation. For the Matagusanos events, changes in locations were larger than for the Pie de Palo events, with a consistent displacement to the west averaging 3.4 km and an average reduction in depth of 2.3 km.

Intermediate-Depth Events

Analysis of the intermediate-depth events illustrates some interesting features of the JHD method and at the same time answers an important question regarding the actual location of these events. In fact, the hypocenters obtained by single-event location seem to indicate a Wadati-Benioff zone with a westward dip (Fig. 7), opposite to the direction of subduction. This anomalous feature was noted and discussed by Smalley and Isacks (1987), who interpreted the dip as evidence for a Moho dipping to the west about 6°.

Because of the apparent westerly dip in the Wadati-Benioff zone, determining accurate locations was as important as the computation of station corrections. For this reason, the selection of events to be jointly located was critical. Tests using only events with epicenters near the Matagusanos fault showed that they were too clustered for joint location purposes. This resulted in large condition numbers for $\mathbf{S}^T\mathbf{S}$ and the loss of numerical stability and required the cancellation of small singular values in the computation of the generalized inverse of $\mathbf{S}^T\mathbf{S}$. As noted below, this cancellation results in substantial mislocation of the events. To avoid this type of problem, we selected events covering a wider area (Figs. 3 and 7), including events out of the network. Because there were accurate *S*-wave arrivals at most stations, the location of the latter events was well constrained. For this selection of events, the four smallest nonzero singular values of $\mathbf{S}^T\mathbf{S}$ were equal to 0.3, 0.6, 0.7, and 10, while the largest singular value was equal to 263. Although these singular values again indicate some clustering of events and a rather large condition number (about 800) for $\mathbf{S}^T\mathbf{S}$, the JHD computations could be carried out keeping the contribution of all nonzero singular values without numerical instability. A useful indicator of the numerical stability of the JHD solution is the sum of the *P*- and *S*-wave stations corrections, which should remain equal to zero if the initial estimates are set

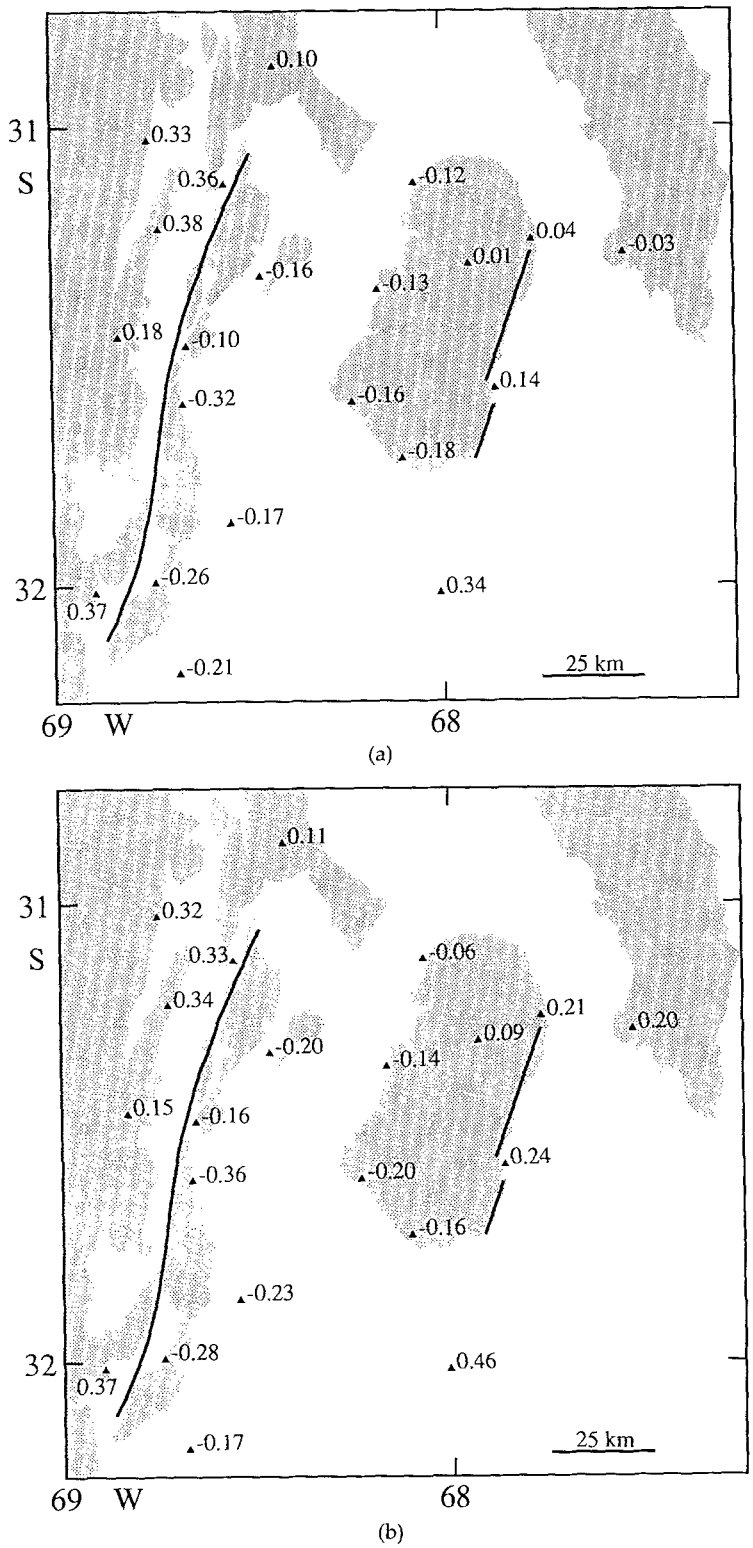

FIG. 5. *P*-wave station corrections (in sec) for the events (a) under Pie de Palo and (b) under and in the vicinity of Pie de Palo. Stations O09, I10, and I18 did not record enough events and were not included in the computations.

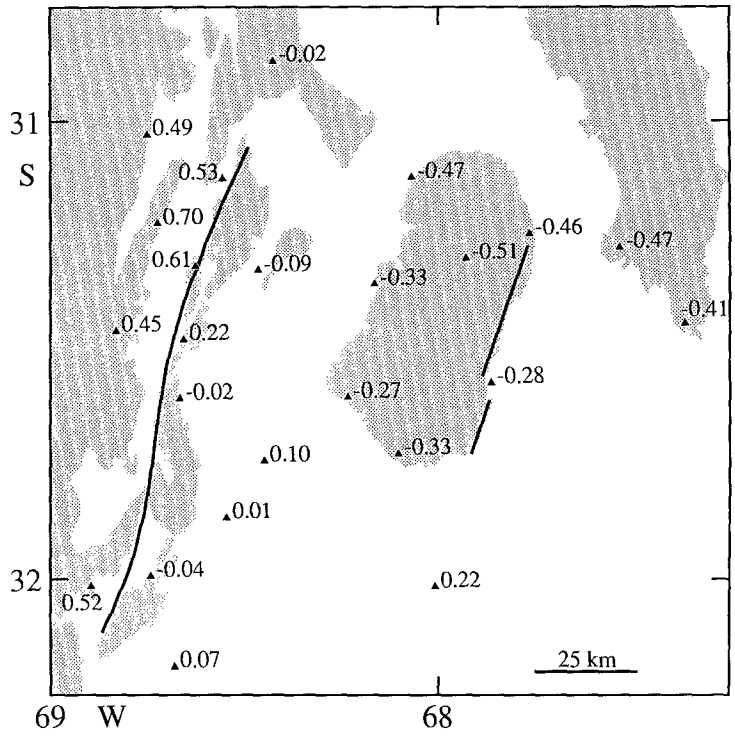

FIG. 6. *P*-wave station corrections (sec) for the Matagusanos events.

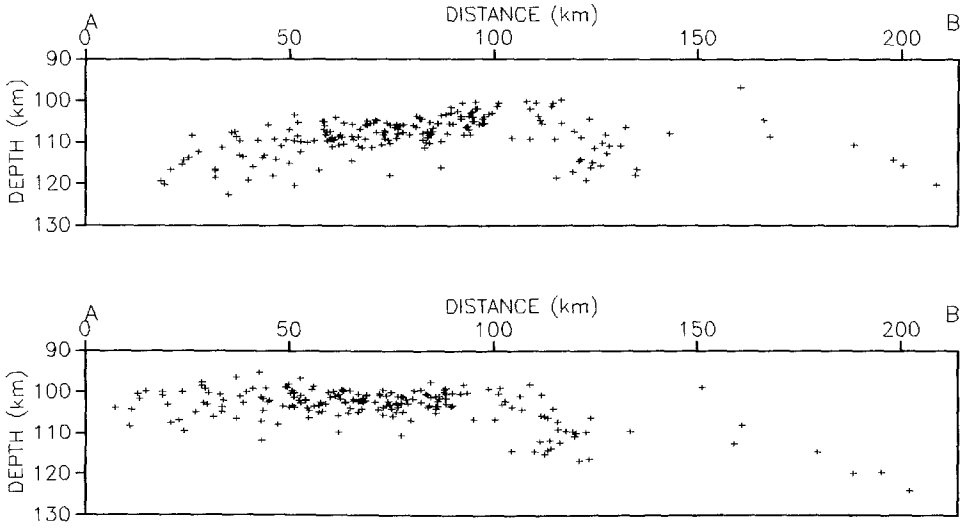

FIG. 7. Depth cross section for the intermediate-depth events (for location see Fig. 3). (*Top*) Single-event locations. (*Bottom*) JHD locations.

equal to zero, as we routinely do (Pujol *et al.*, 1989b). For the intermediate-depth events, the sum of the corrections was equal to 7×10^{-4}, a value close to zero. Keeping the small singular values had an unexpectedly strong effect on the event locations, as the westward dip disappeared and the epicenters moved

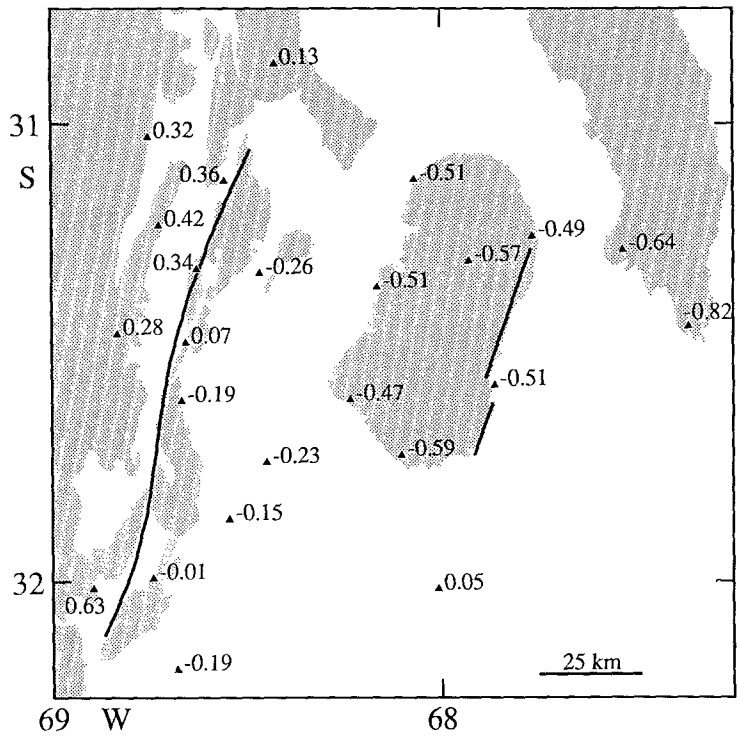

FIG. 8. *P*-wave station corrections (sec) for the intermediate-depth events.

in a westerly direction by almost 10 km (Fig. 7). The average RMS residual decreased from 0.29 to 0.13 sec after relocation. The corresponding *P*-wave corrections (Fig. 8) for the Precordillera stations follow a pattern similar to that obtained using the Pie de Palo events, but for the Pie de Palo stations all corrections are close to -0.5 sec.

To assess the importance of the small singular values, computations were repeated with their contributions cancelled, resulting in station corrections similar in magnitude to those obtained for the Pie de Palo events. However, the hypocenters of the relocated events changed very little with respect to their initial locations. These results confirm that the smallest singular values carry information about absolute locations (Pujol, 1988). The average RMS residual after relocation was equal to 0.14 sec, a value similar to that obtained without the cancellation of singular values. This similarity of RMS residuals demonstrates that small travel-time residuals do not necessarily mean well-located events even in the case of joint location.

For the intermediate-depth events, as well as for the Pie de Palo and Matagusanos events, *S*-wave station corrections were also computed. These corrections follow the pattern of the corresponding *P*-wave corrections, and plots of the *S*-wave versus the *P*-wave corrections show that they are approximately linearly related.

DISCUSSION AND CONCLUSIONS

The station corrections show distinct patterns depending on the events and stations considered and are summarized as follows.

Pie de Palo and Intermediate-Depth Events and Precordillera Stations. Corrections for the stations west of the Matagusanos fault are positive, while for stations east of the fault corrections are negative (except for one positive, but relatively small, value).

Pie de Palo Events and Pie de Palo Stations. Except for station O19, the four stations west of the eastern fault have negative corrections, while for stations east of the fault the corrections are positive. For station O19, the correction is also positive but smaller than for the eastern stations. The magnitude of the positive corrections depends on the events analyzed.

Matagusanos Events and Precordillera Stations. Stations west of the Matagusanos fault have positive corrections, while corrections for stations east of the fault are negative or positive but relatively small with respect to the western stations.

Matagusanos and Intermediate-Depth Events and Pie de Palo Stations. All corrections are negative. For the deeper events the corrections have larger amplitudes and less variation than for the shallower events.

To interpret these observations it should be noted that negative (positive) corrections indicate that actual travel times are shorter (longer) than the computed travel times. This in turn means that negative (positive) corrections correspond to actual velocities that are relatively higher (lower) than the velocities of the flat-layered model used to locate the events. Therefore, the computed station corrections suggest a qualitative laterally varying velocity model with higher velocities between the Matagusanos fault and the eastern edge of Pie de Palo (Fig. 9).

A westerly dipping boundary between fast and slow regions along the eastern edge of Pie de Palo is required to explain the variation in the magnitude of the corrections for stations O17, O18, and O19. The difference in the magnitude of the corrections obtained when only the events directly underneath Pie de Palo (data set 1), and when the Pie de Palo and neighboring events (data set 2) are considered, can be explained by different sampling of a low-velocity zone. For the events in data set 1, the number of rays passing through this zone is smaller than that for the events in data set 2. Therefore, the station corrections corresponding to the second case have to satisfy the travel-time delays that originate in the low-velocity zone. This is achieved by changes in the value of the station corrections and in the event locations. Note that stations O17, O18, and O19 are relatively more affected than the other Pie de Palo stations and that they became more positive, thus reflecting the presence of the lower velocities on the eastern side. Locating the same events with two different sets of corrections and getting basically the same average RMS residual is only possible if the two sets of locations are different. This is what is observed with the events under Pie de Palo. For these events, the epicenters for data set 1 are consistently shifted to the west (0.9 km on average) with respect to the locations they had when the events in data set 2 were jointly located. For most events, the difference in depth is within ± 0.3 km. Although the difference in the location of the two sets of events is relatively small, it shows that the analysis of the uniqueness of the JHD solution based on the singular values of $\mathbf{S}^T\mathbf{S}$ may be somewhat misleading when existing lateral velocity variations are not taken into account.

The Pie de Palo station corrections obtained from the intermediate-depth

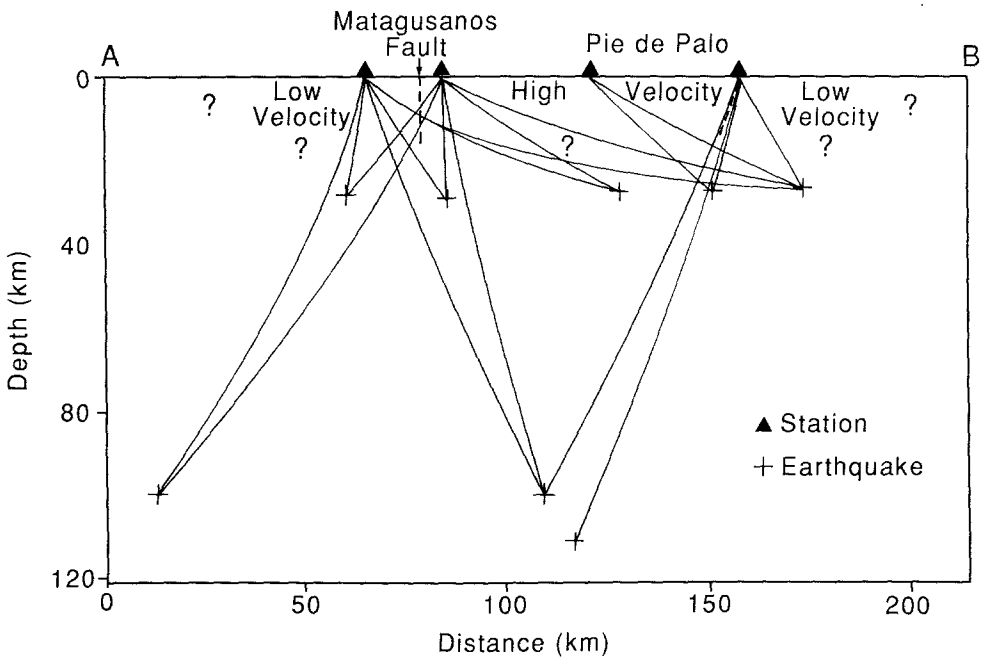

FIG. 9. Qualitative velocity model based on the computed station corrections and schematic ray paths for representative events. Line AB as shown in Figure 3. Velocity boundaries indicated by thick dashed lines. Question marks correspond to unknown velocity boundaries. The relative magnitude of the corrections depend on the regions sampled by the rays.

events help constrain the dip of this boundary, because, as noted before, all these corrections are very close to each other. This indicates that the boundary has to be relatively steep, so that the rays reaching the eastern stations do not sample the low-velocity zone (Fig. 9). Another conclusion to be drawn from the similarity of the corrections is that those obtained for stations O17, O18, and O19 using the Pie de Palo events do not represent localized velocity variations in the vicinity of the stations. Regarding the Pie de Palo stations and the Matagusanos events, the corrections exhibit more variability than for the intermediate-depth events, which may be related to more complicated ray paths, but there is no indication of a systematic difference between the corrections of O17, O18, and O19 and those of the other stations. The postulated boundary agrees with mapped faults on the eastern edge of Pie de Palo and may correspond to the surface along which the mountain block has been uplifted.

The existence of lower velocities to the west of the Matagusanos fault is required by the large difference in the corrections for the stations on both sides of the fault. Furthermore, our results show that the fault is related to some major boundary that juxtaposes rocks having a difference in velocity large enough to affect dramatically the location of the intermediate-depth events. It is not possible, however, to decide whether there is any dip associated with this boundary. To estimate the magnitude of the velocity difference, we use the corrections from the intermediate-depth events, which show that there is an average delay of 0.5 sec across the fault (Fig. 8). Interestingly, the same average difference is obtained for the other three sets of corrections (Figs. 5a,

5b, and 6). Assuming vertical ray paths (which is a good approximation for these events) and a low-velocity zone concentrated in the first layer west of the fault, this delay requires a velocity reduction of 22.7 per cent with respect to the model velocity of 5.88 km/sec. If the whole crust west of the fault is assumed to have lower velocity, then the 0.5 sec delay corresponds to a decrease in velocity of 6.5 per cent with respect to the model RMS velocity, equal to 6.42 km/sec.

The nature of the velocity variation between the Matagusanos fault and Pie de Palo is best estimated by analyzing the Pie de Palo events and the corrections for stations on the western side of Pie de Palo and east of the Matagusanos fault. These corrections are all negative and of similar magnitude, which can be interpreted as an indication that there are no major lateral velocity variations in that area. For the Matagusanos and intermediate-depth events, the corrections for the stations under consideration become rather different, which may be the result of rays that travel almost vertically and that simultaneously sample low and high velocities across the Matagusanos fault (Fig. 9). Additional evidence for small lateral variations comes from the fact that the stations immediately to the east of the fault have corrections that are close to those for stations I07, O07, and O09 (Figs. 5a and b), which are on Pampean basement. Therefore, the Matagusanos fault seems to delineate the eastern boundary of the Pampean basement.

The presence of a significant boundary between the central and eastern Precordillera and the proposed extension of the Pampean basement have important tectonic implications, because they imply that the eastern Precordillera is not simply related to the thin-skinned tectonics responsible for the western and central Precordillera. This conclusion agrees with the recent interpretation of Allmendinger *et al.* (1990) that the eastern Precordillera is formed by the thick-skinned Pampean deformation, although this interpretation is not in full agreement with the seismicity of the area (Smalley *et al.*, 1991).

The proposed model accounts for the general features of the station corrections. Superimposed on the corrections are small-scale velocity variations and local effects, which are beyond the resolution of the JHD method. A good example of this mixing of effects is afforded by station O10, which had corrections consistently smaller than those for the other stations to the west of the Matagusanos fault. This may be attributed to the fact that this station is on dacite, a volcanic rock of higher velocity than that of surrounding sedimentary rocks. Another station strongly affected by local effects is O06, which is on low-velocity valley fill and has a correction that is always positive. Station I11, on the other hand, has a correction always more positive than that of the other stations east of the Matagusanos fault. From the geologic information available, it cannot be decided whether there is a localized low-velocity zone in the vicinity of the station, but from the magnitude and sign of the station correction one may argue that it exists.

The velocity model of Figure 9 was proposed based solely on the pattern of the station corrections (Pujol *et al.*, 1988), but it was recently confirmed by the results of the 3-D velocity inversion of the same shallow data (Matagusanos and Pie de Palo) analyzed here (Pujol *et al.*, 1989a; Chen, 1990; Pujol *et al.*, in preparation). The excellent qualitative agreement between the two sets of results confirms that the JHD technique can provide essential information about the gross features of the velocity structure of an area. Furthermore, in

some circumstances this could be the only information that a given data set can provide. For example, if only the Matagusanos or the Pie de Palo events had been available and the station distribution had been the same, then the 3-D velocity inversion would have not given reliable results over the whole area because of poor resolution. The situation would be worse if only intermediate-depth events had been recorded, as a velocity inversion would not be feasible. In either case, however, the station corrections would have detected the large-scale velocity variations. This suggests that a seismic network should cover an area much wider than the epicentral area, so that the seismic rays can sample the different velocity structures that may exist under the network.

In conclusion, it has been shown that the JHD technique can be extremely useful to detect large-scale velocity anomalies, which is achieved with very little computational effort. Aside from its intrinsic value, this information can be useful in connection with a 3-D velocity inversion. In particular, the distribution and orientation of blocks for the velocity inversion referred to before followed the boundaries of the model of Figure 9. Furthermore, the analysis of the intermediate-depth events has demonstrated the effect of large lateral velocity variations on earthquake location and the need for joint location. Also shown was the importance of the small singular values of matrix $\mathbf{S}^T\mathbf{S}$ and the deleterious effects on event locations introduced by their cancellation.

The application of the technique to shallow and intermediate-depth events in the Andean foreland extended our knowledge of the major structures in the area. In spite of being an oversimplification, the model of Figure 9 has significant tectonic implications. In particular, it suggests that the Matagusanos fault is a major tectonic boundary and indicates the presence of a rather steep boundary dipping to the west on the eastern side of Pie de Palo.

Acknowledgments

We gratefully acknowledge the careful field work of Jim Bollwerk (CERI), T. Cahill (Cornell), and F. Bondoux (ORSTOM), and the assistance of R. Recio, C. Avila, and M. C. Reta (INPRES). The careful review by C. Langer is greatly appreciated. This research was supported by NSF grants EAR 8608301 and EAR 8804925, by ORSTOM, and by the State of Tennessee Centers of Excellence Program.

References

Allmendinger, R., D. Figueroa, D. Snyder, J. Beer, C. Mpodozis, and B. Isacks (1990). Foreland shortening and crustal balancing in the Andes at 30° latitude, *Tectonics* **9,** 789–809.

Aster, R. and R. Meyer (1988). Three-dimensional velocity structure and hypocenter distribution in the Campi Flegrei caldera, Italy, *Tectonophysics* **149,** 195–218.

Baranzangi, M. and B. Isacks (1976). Spatial distribution of earthquakes and subduction of the Nazca plate beneath South America, *Geology* **4,** 686–692.

Baranzangi, M. and B. Isacks (1979). Subduction of the Nazca plate beneath Peru: evidence from spatial distribution of earthquakes, *Geophys. J.* **57,** 537–555.

Bollinger, G. and C. Langer (1988). Development of a velocity model for locating aftershocks in the Sierra Pie de Palo region of western Argentina, *U.S. Geol. Surv. Bull.* **1795,** 1–16.

Chen, Q. (1990). Three-dimensional P- and S-wave velocity structure from inversion of local arrival times: application to data from the Andean foreland in San Juan, Argentina, *M.S. Thesis,* Memphis State University, Memphis, Tennessee.

Chiu, J. M., G. Steiner, R. Smalley, Jr., and A. Johnston (1991). PANDA: a simple, portable seismic array for local- to regional-scale seismic experiments, *Bull. Seism. Soc. Am.* **81,** 1000–1014.

Fielding, E. and T. Jordan (1988). Active deformation at the boundary between the Precordillera and Sierras Pampeanas, Argentina, and comparison with ancient Rocky Mountain deformation, *Geol. Soc. Am. Mem.* **171,** 143–163.

Isacks, B. (1988). Uplift of the central Andean plateau and bending of the Bolivian orocline, *J. Geophys. Res.* **93,** 3211–3231.

Isacks, B. and M. Baranzangi (1977). Geometry of Benioff zones: lateral segmentation and downward bending of the subducted lithosphere, in *Talwani, M., and W. Pitman, Eds., Island Arcs, Deep Sea Trenches, and Back-Arc Basins*, American Geophysical Union, Washington, D.C., 99–114.

Jordan, T., B. Isacks, R. Allmendinger, J. Brewer, V. Ramos, and C. Ando (1983). Andean tectonics related to geometry of subducted Nazca plate, *Geol. Soc. Am. Bull.* **94,** 341–361.

Kadinsky-Cade, K., R. Reilinger, and B. Isacks (1985). Surface deformation associated with the November 23, 1977, Caucete, Argentina earthquake sequence, *J. Geophys. Res.* **90,** 12691–12700.

Langer, C. and G. Bollinger (1988). Aftershocks of the western Argentina (Caucete) earthquake of November 1977: some tectonic implications, *Tectonophysics* **148,** 131–146.

Pavlis, G. and J. Booker (1983). Progressive multiple event location (PMEL), *Bull. Seism. Soc. Am.* **73,** 1753–1777.

Pujol, J. (1988). Comments on the joint determination of hypocenters and station corrections, *Bull. Seism. Soc. Am.* **78,** 1179–1189.

Pujol, J. and R. Aster (1990). Joint hypocentral determination and the detection of low-velocity anomalies: an example from the Phlegraean Fields earthquakes, *Bull. Seism. Soc. Am.* **80,** 129–139.

Pujol, J., Q. Chen, J.-M. Chiu, R. Smalley, Jr., J. Vlasity, D. Vlasity, A. Johnston, J. Bollwerk, G. Steiner, B. Isacks, M. Regnier, J.-L. Chatelain, F. Bondoux, J. Castano, and N. Puebla (1989a). 3-D P- and S-wave velocity structure of the Andean foreland in San Juan, Argentina, from local earthquakes, *EOS* **70,** 1213.

Pujol, J., J. M. Chiu, A. Johnston, and B. H. Chin (1989b). On the relocation of earthquake clusters. A case history: the Arkansas swarm, *Bull. Seism. Soc. Am.* **79,** 1846–1862.

Pujol, J., J. M. Chiu, R. Smalley, J. Vlasity, D. Vlasity, A. Johnston, J. Bollwerk, G. Steiner, B. Isacks, T. Cahill, M. Regnier, J. Chatelain, F. Bondoux, J. Castano, and N. Puebla (1988). Joint hypocentral location of earthquakes recorded in the Andean foreland in Argentina, *EOS* **69,** 1316.

Ramos, V., T. Jordan, R. Allmendinger, S. Kay, C. Mpodozis, J. Cortes, and M. Palma (1986). Paleozoic terranes of the central Argentina-Chile Andes, *Tectonics* **5,** 855–880.

Regnier, M., R. Smalley, Jr., J. M. Chiu, D. Vlasity, J. Pujol, A. Johnston, G. Steiner, J. Bollwerk, J. Vlasity, B. Isacks, T. Cahill, D. Whitman, J.-L. Chatelain, F. Bondoux, J. Castano, and N. Puebla (1988). Analysis of an M_b 5.3 earthquake and its aftershock sequence in the thick-skinned Sierras Pampeanas of the Andean foreland, *EOS* **69,** 1316.

Smalley, R., Jr. and B. Isacks (1987). A high resolution local network study of the Nazca plate Wadati-Benioff zone under western Argentina, *J. Geophys. Res.* **92,** 13903–13912.

Smalley, R., Jr. and B. Isacks (1990). Seismotectonics of thin and thick-skinned deformation in the Andean foreland from local network data: evidence for a seismogenic lower crust, *J. Geophys. Res.* **95,** 12487–12498.

Smalley, R., Jr., J. Pujol, M. Regnier, J.-M. Chiu, B. Isacks, and N. Puebla (1991). Basement seismicity beneath the Andean Precardillera thin-skinned thrust belt and its implications for crystal and lithospheric behavior (submitted for publication).

Smalley, R., Jr., D. Vlasity, J.-M. Chiu, J. Pujol, A. Johnston, G. Steiner, J. Bollwerk, J. Vlasity, B. Isacks, T. Cahill, D. Whitman, M. Regnier, J.-L. Chatelain, F. Bondoux, J. Castano, and N. Puebla (1988). Seismic evidence for active basement deformation beneath the thin-skinned precordillera fold-thrust belt in the Andean foreland, *EOS* **69,** 1316.

Stauder, W. (1973). Mechanism and spatial distribution of Chilean earthquakes with relation to subduction of the oceanic plate, *J. Geophys. Res.* **78,** 5033–5061.

Stauder, W. (1975). Subduction of the Nazca plate under Peru as evidenced by focal mechanisms and by seismicity, *J. Geophys. Res.* **80,** 1053–1064.

Vlasity, J. (1988). A study of seismicity in the subducted Nazca plate beneath the San Juan, Argentina region using high resolution digital data collected by the PANDA array, *M.S. Thesis*, Memphis State University, Memphis, Tennessee.

Volponi, F. (1968). The earthquakes of Mendoza of 21 October 1968 and the structure of the earth's crust, *Acta Cuyana de Ingeniería* **12,** 95–101 (in Spanish).

Volponi, F. (1979). Report of the Argentina-United States binational symposium about the Caucete earthquake of November 23, 1977, Universidad Nacional de San Juan, Instituto de Sismológico Zonda, San Juan, Argentina.

Center for Earthquake Research
and Information
Memphis State University
Memphis, Tennessee 38152
(J.P., J.M.C., R.S., J.V., D.V.)

Institute for the Study of the
Continents Cornell University
Ithaca, New York 14853-1504
(B.I.)

Institut Français de Recherche
Scientifique pour le Développement
en Coopération (ORSTOM)
BPA 5
Noumea, New Caledonia
(M.R., J.L.C.)

Instituto Nacional de Prevención
Sísmica (INPRES)
San Juan, Argentina
(J.C., N.P.)